ASTRONOMY & ASTROPHYSICS
SUPPLEMENT SERIES

Astron. Astrophys. Suppl. Ser. **130**, 465–476 (1998)

Spectral trends in planetary nebulae: The roles of radiative and shock excitation

J.P. Phillips and V. Guzman

Instituto de Astronomia y Meteorologia, Av. Vallarta 2602, Col. Arcos Vallarta, C.P. 44130 Guadalajara, Jalisco, Mexico
e-mail: jpp@udgserv.cencar.udg.mx

Received October 27, 1997; accepted January 19, 1998

Abstract. We have investigated de-reddened spectral line ratios for some 538 planetary nebulae. As a result, it has proved possible to define comparative variations between differing transitions, evaluate the viability of radiative modeling for the generality of nebulae, and assess the importance of shocks in modifying low- excitation line strengths. Whilst most transitions are well represented in terms of radiative excitation, the [OI] λ6300 Å line appears to be appreciably too strong in most of the present sample; a deviation which may arise through shock interaction between the primary outflow shell and enveloping superwind material. Comparison between shock modeling and line excesses also suggests that an appreciable proportion of [SII] λ6716/31 Å emission may arise through shock excitation; a conclusion which, if confirmed, may have serious consequences for nebular density estimations. Some 14 nebulae are identified as likely shock candidates, whilst it is proposed that the majority of bipolar nebulae may also show spectral deviations associated with shock excitation. Line excesses for these latter sources are most consistent with shock velocities $V_s \sim 80 \Rightarrow 100$ km s^{-1}; values which are also comparable to observed wind velocities.

Finally, sources containing FLIERs (Balick et al. 1993) are shown to be confined to highly specific spectral regimes; a result which permits us to identify three further possible FLIER sources, and propose characteristic line ratio diagnostics for the further discovery of such features.

Key words: survey — ISM: planetary nebulae — ISM: jets and outflows — shocks waves

1. Introduction

The low-excitation transitions of planetary nebulae have long constituted a thorny problem for nebular spectral analysis and model simulations. Thus, whilst the intensities of intermediate to high excitation lines can often be represented in terms of quite simple nebular models (e.g. Aller 1982), lower excitation line simulations are frequently grossly in error (cf. Köppen 1983; Middlemass 1990); a disparity which has only partially been alleviated through recent use of more realistic (non-homogeneous, non-spherically symmetric) source structures (Hyung et al. 1994, 1995; Hyung & Aller 1996). Whilst the reasons for these differences are far from clear, it appears likely that "excess" components of emission are associated (in part) with micro-filamentary structures and clumps (Hyung et al. 1994, 1995; Köppen 1979; Boeshaar 1974; Hyung & Aller 1995).

A further complicating factor relates to the possible contribution of shocks; a process which is believed to be important for explaining certain small (e.g. Balick et al. 1993, 1994; although see later) and larger scale nebular structures (Cuesta et al. 1993, 1995; Balick et al. 1983; Icke & Preston 1989; Icke et al. 1992), and would likely result in enhanced low-excitation transitions (Shull & McKee 1979; Raymond et al. 1989; Hartigan et al. 1987). Distinctive shock emission signatures have already been noted in for instance CRL 618, M2-56 (Goodrich 1991), KjPn 8 (Lopez et al. 1995) and a variety of other sources (Bohigas 1994; Balick et al. 1993, 1994; Meaburn & Walsh 1980a, 1980b; Rowlands et al. 1994; Trammell & Goodrich 1996), although the general prevalence of shocks (and their importance in explaining lower excitation line strengths) remains far from clear.

In the following, we shall analyse a broad range of published optical spectra with the aim of evaluating trends in (de-reddened) line emission for some 538 nebulae. These are compared with the variations expected for radiative and shock excitation models in an attempt to evaluate the importance of collisional excitation; the extent to which low excitation line anomalies are representative of planetary nebulae (PN) in general; and finally, to determine

Send offprint requests to: J.P. Phillips

the evolution in relative selected line ratios as a function of nebular radius.

2. Observational and model data

For the purposes of this analysis we have compiled in excess of 2700 line intensities for the transitions of [OII] λ3729/6 Å, [OIII] λ4959/5007 Å, [NI] λ5200 Å, [OI] λ6300 Å, [SII] λ6716/31 Å, [SIII] λ9532 Å, HeI λ5876 Å, and HeII λ4686 Å, using 807 spectra derived from Kaler et al. (1996; a catalogue which is in turn based upon data from in excess of 450 referenced sources); where following standard convention, the various line intensities $I(\mathrm{X})$ are quoted in terms of the normalised function 10^2 $I(\mathrm{X})/I(\mathrm{H}\beta)$. Since shocks may be confined to isolated regimes within the nebular shells (see later), we have also included spectra taken at multiple locations within the same source.

The spectra have subsequently been dereddened using the extinction measurements by Tylenda et al. (1992) in combination with the extinction curve of Savage & Mathis (1979). Note, in this latter case, that extinctions based upon radio/Hβ measurements appear to be particularly susceptible to uncertainties, and have not been included in the present analysis. Similarly, results acquired at the Observatoire de Haute Provence appear to be prone to error, and have been employed sparingly.

From comparison with independent extinction measurements (Tylenda et al. 1992) it appears that typical internal errors do not exceed $\Delta C \sim 0.6$ mag, which would generate corresponding logarithmic errors in de-reddened line ratios $\Delta\log$[OII] ~ 0.17 and $\Delta\log$[SII] ~ 0.19 (errors in [OIII] would be significantly less, and in [SIII] somewhat larger). Similarly, errors in line ratio measurements are unlikely to exceed 30%, implying logarithmic errors ≤ 0.1.

Finally, the resulting corrected line strengths have been correlated with nebular radii from Cahn et al. (1992) with the aim of evaluating evolutionary variations in line strength. Similarly, the observed trends are compared to bow- and planar-shock results deriving from Hartigan et al. (1987) and Shull & McKee (1979), and a variety of radiative modeling results from Gruenwald & Viegas (1992).

The latter analysis includes line ratio estimates for various lines-of-sight through the model nebular shells; a procedure which differs from most prior evaluations, and parallels the procedures employed in acquiring the present observations. We have included modeling for central star temperatures 3.09 10^4 K $\leq T_* \leq$ 5 10^4 K, densities 10^2 cm^{-3} $\leq n_\mathrm{e} \leq 10^3$ cm^{-3}, and abundances $1/30 \leq Z/Z_0 \leq 1$. Taking account of the evolutionary tracks of Schonberner et al. (1979, 1981, 1983), and the mean shell expansion velocities of Phillips (1989), it is apparent that model ratios conform most closely to radiatively-limited shells with radii $R < 0.1$ pc.

A selection of figures resulting from this analysis is illustrated in Figs. 1 and 2.

3. Spectral trends in the general population

3.1. Characteristics of the [OI] transition

It is apparent from both narrow and broad-band imaging of planetary nebulae that shell structures are often extremely complex, whilst fine-scale components (whether clumpy or filamentary) may be associated with anomalous enhancements in [OI] (see references cited in Sect. 1). The present results suggest that some such deviation from normal trends must apply for the large majority of sources, with [OI] in particular (Figs. 1c, d, f, h) lying substantially outside the range defined through the modelling of Gruenwald & Viegas (1992): observed values are in almost all cases appreciably in excess of simulated results. It therefore appears that the present results confirm for the generality of nebulae what has long been known for individual sources.

A diagram representing the excess in line ratios for [OI] and other transitions is illustrated in Fig. 3 (see the trend designated "OBSERVED"), wherein we indicate a parameter $R(\mathrm{GEN}) = \langle\log(I_\mathrm{G})\rangle - \langle\log(I_\mathrm{M})\rangle$ for the general population of sources; where $\langle\log(I_\mathrm{M})\rangle$ represents the mean logarithmic line ratio for the radiative models combined, $\langle\log(I_\mathrm{G})\rangle$ is the corresponding parameter for the observed nebular sample, and bipolar nebulae have been excluded (see the further discussion in Sect. 4.1). We have also corrected R([OIII]) for use of inappropriately low model central star temperatures, as discussed in Sect. 4. Broadly speaking, therefore, R(GEN) is an indication of the proportionate excess in line ratios over those anticipated through radiative modelling.

It is apparent that excesses in [OI] represent by far the most serious departures from modelling of any of the transitions considered here. This, in part, is likely to be the result of low [OI] model line ratios, such that small excesses in all lines would lead to disproportionately large effects in this particular transition. Indeed, the evaluation of a median excess parameter $\langle\Delta I_\mathrm{D}\rangle = \langle I_\mathrm{G}\rangle - \langle I_\mathrm{M}\rangle$ suggests that the trends illustrated in Fig. 3 are consistent with a similar excess in all transitions - a species of "veiling" over and above that arising through normal radiative excitation. How could such a component arise?

One possible indication is afforded through the work Reay et al. (1988) and Phillips et al. (1992), where it is noted that [OI] line intensities are proportional to the intensity of shocked $\lambda = 2.1$ μm H$_2$ $S(1)$ emission. One plausible explanation, therefore, is that we are witnessing a small shock excess at the HI/HII interface of optically thick sources, or over the surfaces of neutral condensations within the primary ionised mass.

Under these circumstances, and given that $I_\mathrm{M} = {}^\mathrm{R}I_\mathrm{L}/{}^\mathrm{R}I_\beta$, and $I_\mathrm{G} = ({}^\mathrm{R}I_\mathrm{L} + {}^\mathrm{R}I_\mathrm{S})/({}^\mathrm{R}I_\beta + {}^\mathrm{S}I_\beta)$, then $\langle\Delta I_\mathrm{D}\rangle$

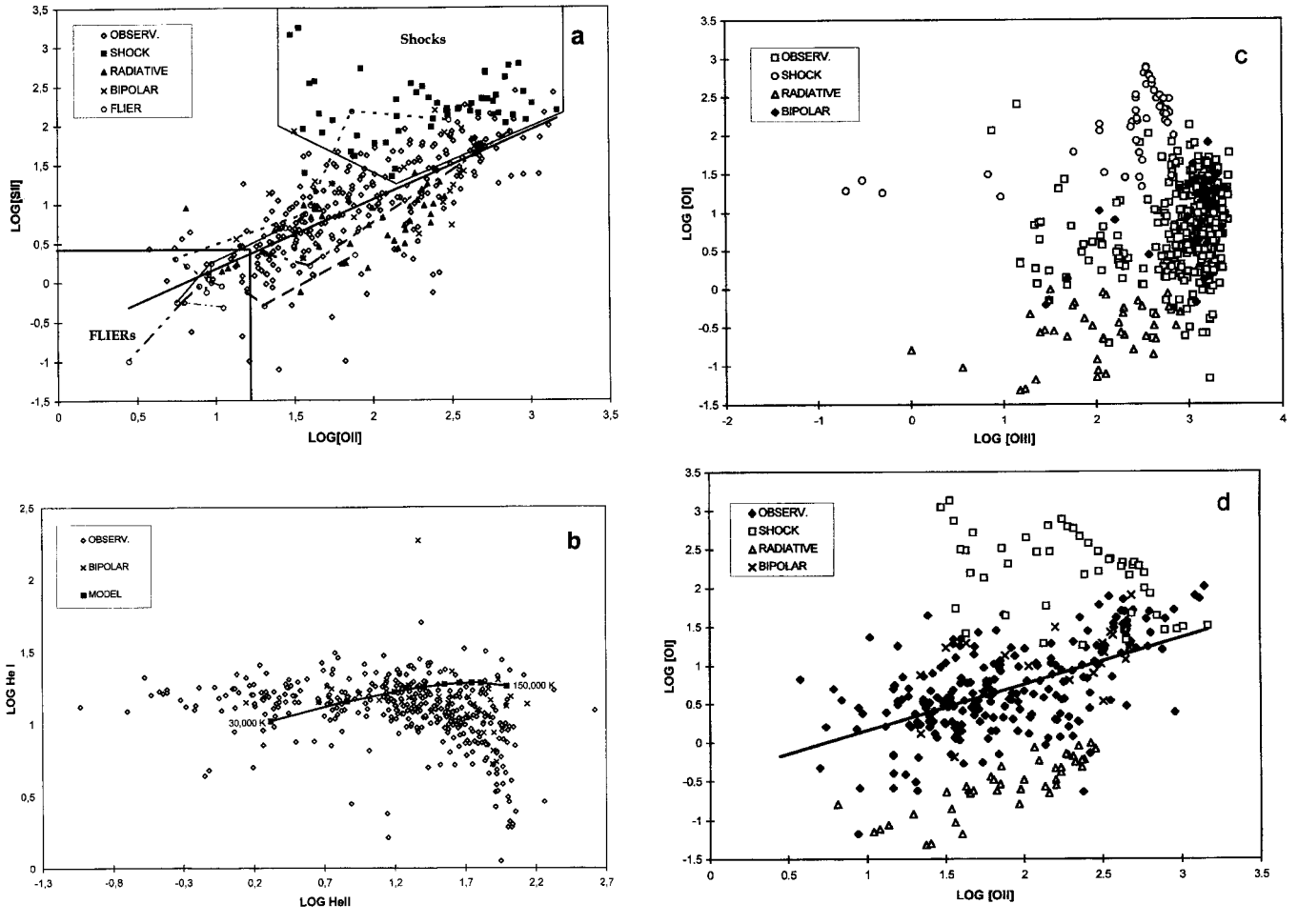

Fig. 1. a) Logarithmic variation of [SII]/Hβ with respect to [OII]/Hβ, where we have indicated separately the results corresponding to "normal" planetary nebulae (denoted "OBSERV." in the internal caption), bipolar sources, shock and radiative models, and sources containing FLIERs. The primary regimes corresponding to shock modeling and FLIERs are also indicated separately. Multiple measures of individual FLIER sources are connected by dashed lines, whence it is apparent that NGC 7009 (- - - - -) and NGC 6543 (— - — - — -) are associated, in particular, with a broad range of line ratios. The single solid diagonal line corresponds to the least squares regression trend for non-bipolar sources

may be equated with $({}^{\rm S}I_{\rm L} - {}^{\rm R}I_{\rm L}({}^{\rm S}I_\beta/{}^{\rm R}I_\beta))({}^{\rm R}I_\beta + {}^{\rm S}I_\beta)^{-1}$; where I_β is the Hβ emission intensity, $I_{\rm L}$ is the intensity of the transition under investigation, and superscripts R and S refer respectively to the radiative and shock terms. Where ${}^{\rm S}I_\beta \ll {}^{\rm R}I_\beta$ and ${}^{\rm R}I_{\rm L} \leq {}^{\rm S}I_\beta$ then $\langle \Delta I_{\rm D} \rangle \approx {}^{\rm S}I_{\rm L}/{}^{\rm R}I_\beta$. In other words, $\langle \Delta I_{\rm D} \rangle$ for [OI] will be broadly proportional to the shocked line intensity. Note, in this respect, that force-fitting of observed [OI] line ratios to a mix of shock and radiative modelling would imply values ${}^{\rm S}I_\beta/{}^{\rm R}I_\beta \sim 0.06$ for shock velocities $V_{\rm s} = 45$ km s^{-1}; a ratio which decreases still further as $V_{\rm s}$ increases.

Inspection of the shock results of Raymond et al. (1988) and Hartigan et al. (1987) reveals that a variety of specifications might satisfy required excess characteristics, including models I20⇒I80, A100, D100 and bow shock models 3 and 4. These are characterised by fairly modest velocities $V_{\rm S} \sim 20 \Rightarrow 100$ km s^{-1}; comparable to [OIII]/HI expansion velocities $V_{\rm exp} \sim 25$ km s^{-1} in normal PN (e.g. Phillips 1989; although note that [OII]/[NII] velocities (characteristic of the nebular peripheries) are typically $\sim 60\%$ larger).

Although the excess trends, observed expansion velocities and shock modelling appear therefore to offer a consistent scenario, care must be taken in the interpretation of such results; in particular, the synthetic data used to assess $\langle I_{\rm M} \rangle$ are far from representing an appropriate balance of models. Thus, although the radiative modelling appears to simulate observed trends tolerably well (see later), slight errors in $\langle I_{\rm M} \rangle$ would have a disproportionate effect upon $\langle \Delta I_{\rm D} \rangle$ in all excepting the [OI] results.

A more interesting question, under these circumstances, is whether the very much more greatly enhanced [OI] line ratios are consistent with plausible shock

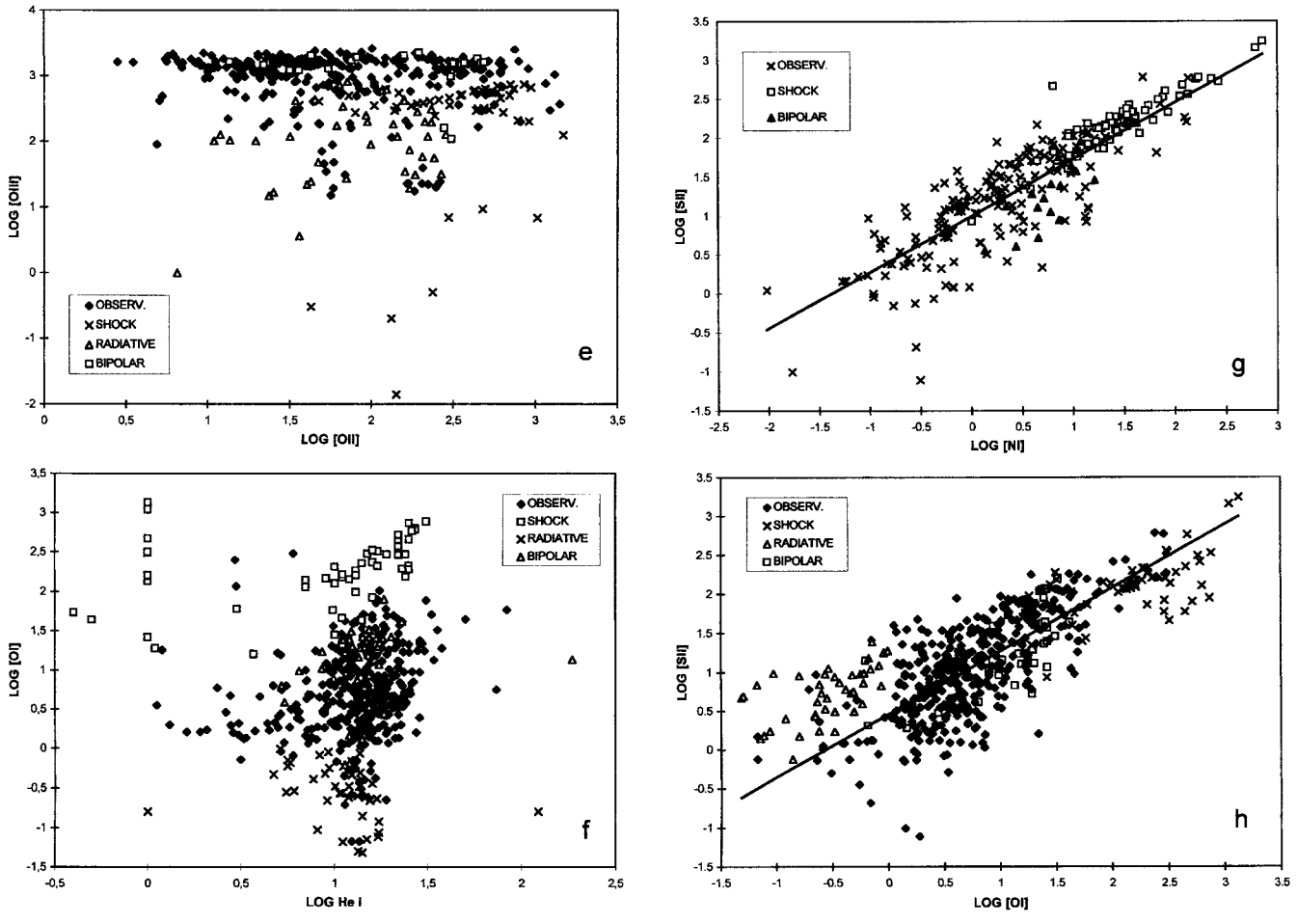

Fig. 1. b) Logarithmic variation of HeI/Hβ with respect to HeII/Hβ, where we have included the trend expected for radiative line excitation in radiatively-bound sources (see text for details). Commencing from the extreme left, model points correspond to central star temperatures of 30 000 K, 40 000 K, 50 000 K, 60 000 K, 70 000 K, 80 000 K, 90 000 K, 100 000 K, and 150 000 K. The range in scatter of the results is significantly less than for the transitions illustrated in Fig. 1a

modelling. To investigate this, we note that for a shock extending uniformly over the surface of a spherical nebula

$$\frac{^{\rm s}I({\rm OI})}{^{\rm R}I({\rm H}\beta)} = \frac{7.8\ 10^2 \left[\frac{^{\rm s}I({\rm OI})}{^{\rm s}I({\rm H}\beta)}\right] \left[\frac{^{\rm s}F({\rm H}\beta)}{10^{-4}{\rm ergs\ cm^{-2}s^{-1}}}\right]}{n_{\rm e}^2 (R/{\rm pc})\varepsilon}$$

for case B radiative conditions, where ε is the nebular filling factor, $n_{\rm e}$ is the electron density, and $^{\rm s}F({\rm H}\beta)$ is the Hβ flux emerging from the shock front. Given a proton number density

$$n_{\rm p} = \frac{3\ M}{4\pi R^3 m_{\rm H} \varepsilon \mu}$$

where M is the shell mass, and μ is the mean atomic mass per proton, and taking $^{\rm s}F({\rm H}\beta) = U(n_{\rm e}/10^2\ {\rm cm}^{-3})$ then gives

$$\frac{^{\rm s}I({\rm OI})}{^{\rm R}I({\rm H}\beta)} = \frac{3.86[^{\rm s}I({\rm OI})/^{\rm s}I({\rm H}\beta)][R/{\rm pc}]^2 U}{M/M_0}$$

where U is a steeply varying function of shock velocity $V_{\rm S}$ ($U \propto V_{\rm S}^{3.5}$), and we assume pre-shock densities to be comparable to $n_{\rm e}$. For representative values $M \sim 0.1\ M_\odot$, $R \sim 0.1$ pc and employing a value $U \cong 0.22$ appropriate for $V_{\rm s} \sim 40$ km s^{-1} then yields $^{\rm s}I({\rm OI})/^{\rm R}I({\rm H}\beta) = .038$; a ratio which increases to .053 for $V_{\rm s} \sim 50$ km s^{-1} ($U \cong 0.54$). For comparison, the observed value of $\Delta I_{\rm D}([{\rm OI}])$ based on logarithmic mean estimates (i.e. $\log\langle\Delta I_{\rm D}([{\rm OI}])\rangle = \langle\log(I_{\rm M}([{\rm OI}])\rangle \log(10^{{\rm R}([{\rm OI}])} - 1)$) is of order 0.052. It is therefore clear that much of the observed emission may indeed be explicable through such a mechanism. Indeed, the viability of such a model may be even greater than supposed above, since a variation in nebular mass $M \propto n_{\rm e}^{\gamma}$, $\gamma = -1 \Rightarrow -0.7$ (e.g. Boffi & Stanghellini 1994; Pottasch 1984) would tend to proportionately enhance [OI] in smaller nebulae.

In contrast, the trend towards smaller values of $V_{\rm exp}(R)$ with decreasing R (e.g. Phillips 1989) might be expected to work in the reverse direction, and lead to corresponding decreases in [OI] shock excesses; a factor which may be responsible for the shallow secular variations in [OI]/Hβ noted in Sect. 3.2.

Finally, the theoretical trends for a range of transitions and velocities are presented in Fig. 3. It can be seen

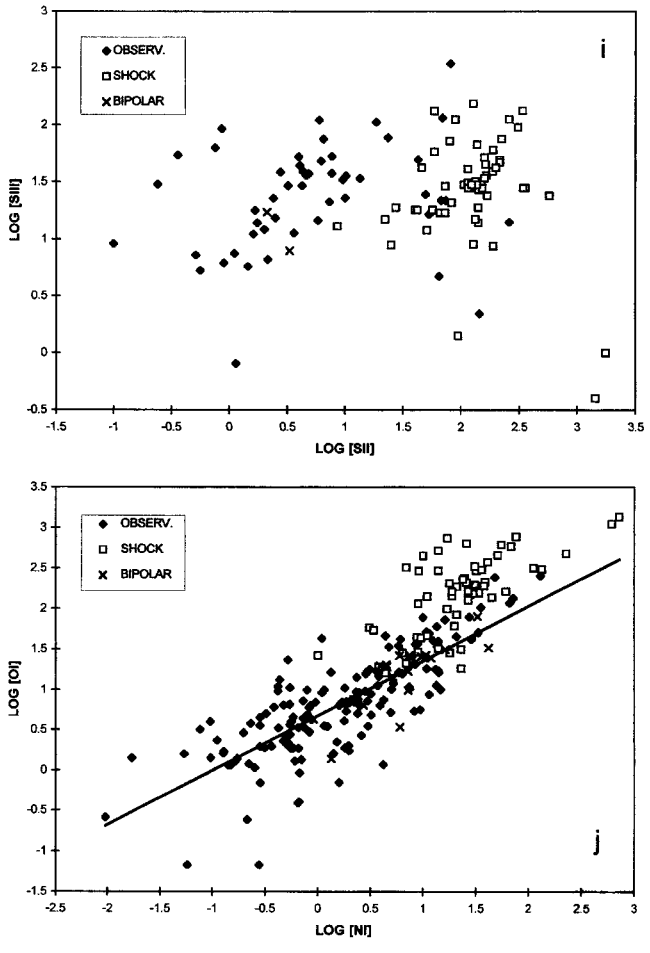

Fig. 1. c-j) Comparative logarithmic trends for a selection of nebular transitions, where the solid diagonal lines again correspond to least-squares regressions for non-BPN sources

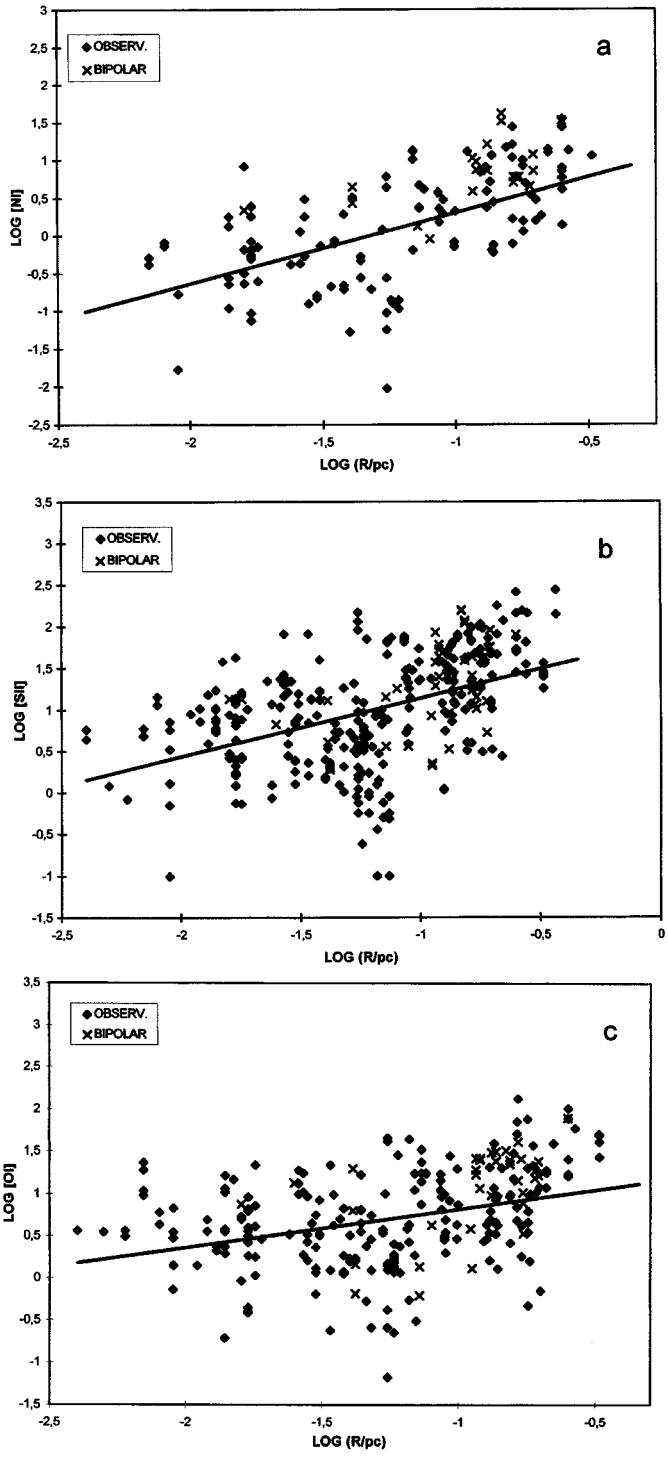

Fig. 2. a-c) Line ratio variations as a function of nebular radius for [NI], [SII] and [OI], where the solid lines correspond to least squares regression trends. Note that most of these variations may be attributed to a quantal increase in line strength for density bound sources ($R \geq 0.1$ pc)

that shock modelling predictions are more than adequate, and accommodate a good proportion of the excess in [SII] which, on this basis, would appear to be shock enhanced by a factor ~ 2. Such a result may have severe consequences for our understanding of nebular densities, since it is apparent that [SII] line ratios would be to some degree representative of compressed post-shock regimes, and imply higher densities than are appropriate for the primary nebular shells.

A further possible source for such trends may arise through UV shadowing, appreciable ionisation stratification, and charge exchange reactions in zones of partial ionisation. Such mechanisms may not, in fact, be entirely divorced from the process of shock excitation considered above, since Rayleigh-Taylor and Kelvin-Helmholtz instabilities would be expected to lead to frontal irregularities, and the possible development of globular neutral condensations within the primary ionised zones (cf. Capriotti 1973). Whether such features could account for the "veiling" excesses noted above is, however, far from clear, and requires further analysis.

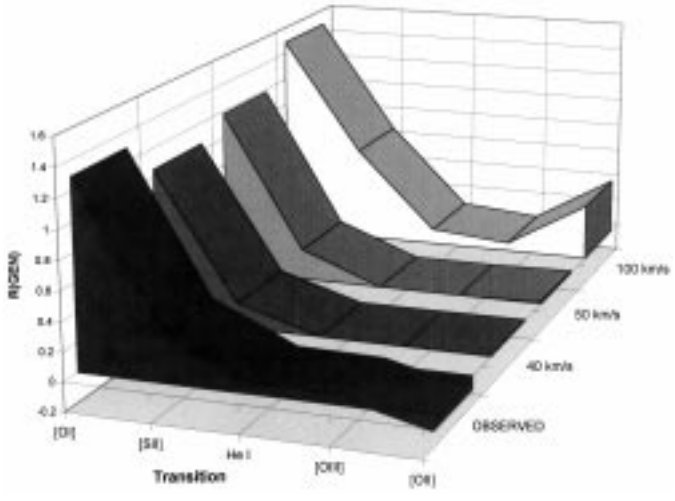

Fig. 3. Observed variation of R(GEN) as a function of transition, together with comparative predictions for selected planar shock models

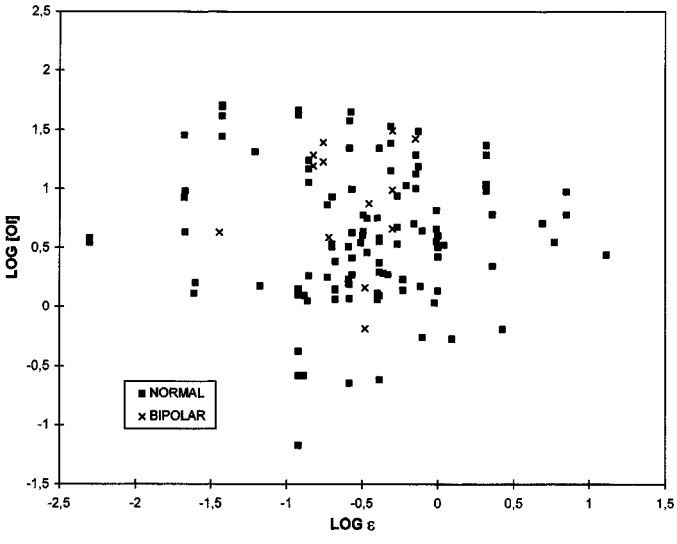

Fig. 4. Variation of [OI]/Hβ with respect to the nebular filling factor ε

Finally, we have noted that low-excitation emission appears often to be associated with small-scale condensations and filamentary structures (see for instance the spectro-morphological studies of Phillips & Reay (1980) and Boeshaar (1974), high resolution imaging of nearby nebulae (e.g. NGC 7293, NGC 6543; e.g. Harrington 1995; O'Dell & Handron 1996), and the line modelling analyses of Hyung et al. (1994, 1995), Köppen (1979), Boeshaar (1974) and Hyung & Aller (1995). It is therefore pertinent to ask whether the strength of the [OI] transition may be related to the degree of fragmentation of the primary shell. More specifically, is there a correlation between [OI] line strengths and the nebular filling factor ε? To investigate this question, we have plotted the variation of I([OI]) against values of ε derived from Boffi & Stanghellini (1994), Kingsburgh & Barlow (1992), Kingsburgh & English (1992) and Mallik & Peimbert (1988) (Fig. 4; where we have adopted averaged values of ε where multiple estimates are available). Cursory inspection suggests that there is little correlation between the parameters. Whilst [OI] excitation may be associated with nebular condensations, therefore, it would appear that such emission is only superficially related to primary shell fragmentation.

3.2. Radiative excitation of ionic transitions

In contrast to [OI], the other transitions investigated here appear to follow radiative modelling trends tolerably closely. We briefly review the characteristic line ratio trends for the remaining transitions:

1) Trends in [SII], [OII] and HeI line ratios appear broadly consistent with radiative modelling (Figs. 1a, f; although note comments concerning [SII] in Sect. 3.1).

2) Power-law trends exist between the transitions [NI], [OI], [OII], and [SII] (see Figs. 1a, d, g, h and j for representative examples, and Table 1 for a summary of various least-squares fits; where $Y = MX + C$, and r^2 is the correlation coefficient). In comparison, trends between the radiative modelling results for [SII] and [OII], and HeI and [OII] appear closely similar in terms of absolute intensities and gradients

Table 1. Least squares regression analysis for spectral line ratios

Y	X	C	M	r^2
LOG[OI]	LOG[NI]	+0.70	0.68	0.65
LOG[SII]	LOG[NI]	+0.99	0.71	0.63
LOG[SII]	LOG[OII]	−0.74	0.90	0.56
LOG[SII]	LOG[OI]	+0.46	0.81	0.51
LOG[OI]	LOG[OII]	−0.45	0.61	0.33
LOG[SIII]	LOG[OII]	+1.20	0.13	0.04
LOG[NI]	LOG[OII]	−1.90	1.01	0.57
LOG[NI]	LOG(R/pc)	+1.43	1.04	0.37
LOG[SII]	LOG(R/pc)	+1.88	0.73	0.23
LOG[OI]	LOG(R/pc)	+1.38	0.52	0.15

Given that many of these line intensities increase with increasing source radius (see Sect. 4 below), the trends also correspond to an evolutionary sequence in which younger nebulae (high densities, lower central star temperatures) are located to the lower left of Figs. 1, and older nebulae are to the upper right.

3) Comparison between theoretical and model results for [NI], [OI], [OII], and [SII] reveals that the levels of scatter are comparable. Much of the theoretical scatter derives from the range of parameters T_e, n_e, and Z employed for the radiative modelling, as well as through the contributions of differing lines-of- sight through the nebular shells. This, in turn, underlines the necessity of employing multiple line-of-sight analyses for any radiative investigation

of nebular line strengths; a factor not always appreciated in previous analyses.

Note that the size of scatter exceeds probable errors (Sect. 2) by a factor ~ 5.

4) Although correlation coefficients are relatively low, there appears to be evidence for statistically significant variations in [OI], [SII], and [NI] line intensity with nebular radius (Fig. 2). This does not apply for higher excitation transitions such as [SIII], HeII, [OIII] and He I. The radial gradient for [NI] appears significantly greater than for any other ion, whilst gradients for [OI] and [SII] are comparable.

Such trends would be at variance with radiative modelling of ionisation-bound nebulae, given likely evolutionary trends in T_* and n_e. On the other hand, careful perusal of these figures suggests that much of the apparent variation may arise from a jump in low-excitation line-strengths close to $R = 0.1$ pc, by typical factors of between 0.5 and 0.75 dex; that is, as a result of the transition from radiatively-bound to density-bound ionisation structures.

5) [SIII] intensities were not modelled by Gruenwald & Viegas (1992), although they appear to be broadly comparable to those expected through shocks (Fig. 1i).

6) The variation of HeI with HeII differs from most other trends in revealing a relatively constant ratio $I(\mathrm{HeI})/I(\mathrm{H}\beta)$ up to the limiting value $\log(10^2\ I(\mathrm{HeII})/I(\mathrm{H}\beta)) \sim 2$, after which there is some down-turn in ratios. Such trends are broadly consistent with radiative analyses, as noted from the model results illustrated in Fig. 1b; where we have assumed model nebulae to be optically thick, spherical and homogeneous, with typical densities $n_e = 10^4$ cm^{-3}, and electron temperatures $T_e = 10^4$ K (the relevant emission parameters are insensitive to these parameters). We have also assumed $n(\mathrm{He})/n(\mathrm{H}) = 0.115$, case B conditions, a range of stellar temperatures $3\ 10^4\ \mathrm{K} \leq T_* \leq 1.5\ 10^5$ K, and adopted a blackbody approximation to the stellar continuum. Ratios refer to lines of sight through the nebular cores.

The downturn in $I(\mathrm{HeI})/I(\mathrm{H}\beta)$ for large values of $I(\mathrm{HeII})/I(\mathrm{H}\beta)$ occurs for high central star temperatures, and applies (in particular) to density-bound structures.

Finally, note that the similarity of HeI and Hβ emission regimes for large ranges of central star temperature, and the relative insensitivity of emission coefficients to n_e and T_e would lead to comparable HeI line ratios irrespective of the mode of spectral sampling. This, in large part, is probably responsible for the reduced scatter in HeI compared to [SII] and other intermediate excitation transitions.

7) The low scatter, invariant trend of [OIII] line ratios (Figs. 1c, e) is also broadly consistent with the distribution expected for radiative line excitation. For very much the same reasons as were cited for HeI above, [OIII]/Hβ ratios are expected to be reasonably consistent over a broad range of central star temperatures, and as a function of projected shell location.

The failure of the radiative modelling to reproduce these trends appears to arise, in part, from a sensitivity in [OIII]/Hβ ratios to low central star and nebular temperatures; both sets of parameters are smaller (in certain models) than would be appropriate for the spectral data base investigated here.

4. Shock excitation of the nebular spectra

Given recent evidence for high velocity winds in planetary nebulae (e.g. Cuesta et al. 1995), and for the formation of jets and highly collimated flows at various stages of PN evolution (cf. references cited in Sect. 1), it has become apparent that many planetary nebulae are likely to display a range of shock related activity. Thus, for instance, Bohigas (1994), Goodrich (1991), Trammell & Goodrich (1996) and Lopez et al. (1995) have noted spectral signatures consistent with shocks extending throughout large fractions of the nebular ionised regimes, whilst Cuesta et al. (1993, 1995) have found that the spatio- kinematic structures of certain sources are consistent with shock interaction between interior winds and external (superwind) envelopes. These latter models (see also Balick et al. 1987; Icke & Preston 1989; Icke et al. 1992) also bear a striking resemblance to the radiative modelling structures of Hyung et al. (1994, 1995) and Hyung & Aller (1996), and it is pertinent to ask whether such radiative analyses should not also make allowance for components of shock excitation.

Finally, recent high resolution imaging has revealed that the helical structure of NGC 6543 may arise through interaction between precessing jets and the primary shell (Harrington 1995); whilst high velocity condensations ("FLIERs") are also likely to be associated with strong shocks (although Balick et al. (1994) have voiced doubts concerning the viability of this mechanism; see later).

It is apparent, therefore, that shock excitation may dominate emission in certain post-main-sequence sources, and it is relevant to ask whether the present work offers any guide to identifying further such nebulae.

In fact, and apart from CRL 618, very few sources can be unambiguously identified as being shock-excited; the level of dilution by radiative components of emission appears in most cases to be appreciable. Thus, whilst [OI]/Hβ line ratios are higher than would be anticipated from radiative modelling, and may be partially enhanced by shocks (see Sect. 3.1), they are distinctly smaller than would be expected through shock modelling (a disparity which reflects the predominance of radiatively excited Hβ emission). Similarly, whilst [OIII] line strengths are larger than predicted through shocks, [NI] intensities appear to extend well into the shock regime of Fig. 1j; although as part of a trend between [OI] and [NI] which extends primarily outside of the shock zone.

Various nebulae may, nevertheless, represent strong candidates for possible shock excitation, including the

Table 2. Candidate shock excited nebulae

Source	Spectral Regime	Source	Spectral Regime
BV 1	[OII]/([SII][NI])	NGC 650	[SII]/[OII]
CRL 618	[NI]/([OI][OII][OIII]), [SI I] /([OI][OIII]),[OI]/HeI	NGC 2899	[NI]/[OI]
ESO 21602	[NI]/[OI]	NGC 6720	[NI]/([OIII][OII])
He 2-15	[NI]/[OI]	NGC 6853	[NI]/([OI][OII][OIII]), [SII]/([OI][OII])
He 2-111	[OII]/([NI][SII])	NGC 7019	[SII]/[OII]
M 2-51	[NI]/[OI]	NGC 7293	[NI]/[OII]
M 2-56	[OI]/([SII][NI])	YM 29	[SII]/[OII]

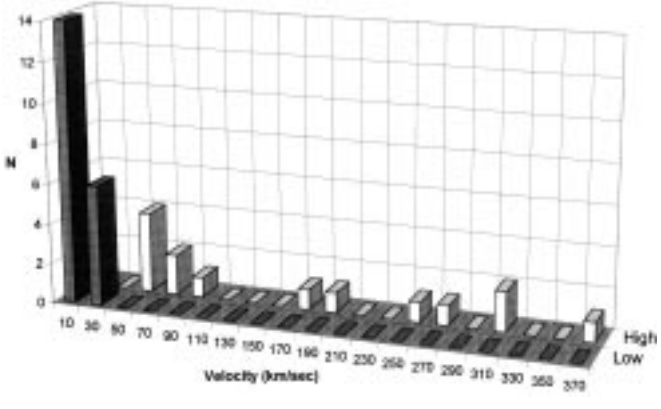

Fig. 5. Histograms of observed expansion velocities in bipolar nebulae, where we have indicated both the primary shell velocities (Low), and the velocities associated with accelerated winds (High)

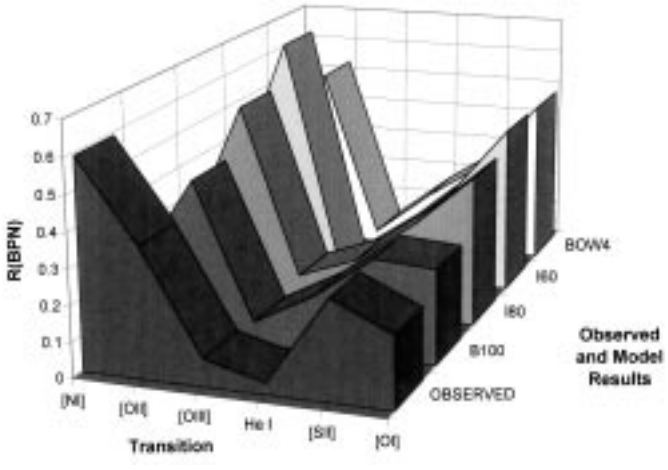

Fig. 6. Variation of observed values R(BPN) as a function of transition, wherein are also indicated the trends expected for a variety of shock models

ubiquitous CRL 618 and some 13 other sources (Table 2, where spectral identification regimes are also indicated; [SII]/([OI][OIII]) would imply detection in the [SII]−[OI] and [SII]−[OIII] shock regimes). Certain of these sources have previously been identified as likely shock candidates (viz. CRL 618 and M2-56; Goodrich 1991), and/or possess strong shock excited H_2 $S(1)$ emission (e.g. NGC 6853, NGC 6720, NGC 2440, NGC 650, NGC 2899 and CRL 618 (e.g. Zuckerman & Gatley 1988; Kastner et al. 1994, 1996; Webster et al. 1988)). In addition, a large proportion also possess bipolar morphologies; and these (with their typically high velocities of outflow) constitute one of the most likely subcategories in which such emission might be observed. We have therefore indicated separately in the figures all of those nebulae for which the observed morphology is bilobal.

4.1. Bipolar sources

Apart from the sources cited individually in the previous section, it appears that the majority of BPN fall outside of the shock regimes in Fig. 1; although there are, nevertheless, various trends to suggest that shock excitation may be important for the group as a whole.

In the representation of [NI] against [OI] (Fig. 1j), for instance, it is apparent that 74% of BPN fall into the shock regime, whereas for the more general nebular sample the proportion is 28%. Although this may be partly explicable in terms of enhanced N abundances (viz. Peimbert & Torres-Peimbert 1983; Corradi & Schwartz 1995), such contributions are unlikely to account for all of the bias. Similar trends (although perhaps less distinctive) are to be found in plots of [OI] versus [OII] (Fig. 1d), [OI] versus HeI (Fig. 1f), and so on.

These disparities are also illustrated in a slightly differing way in Fig. 6, where following the prescription in Sect. 3.1. we have defined a function $R(\mathrm{BPN}) = \langle \log(I_{\mathrm{BPN}}) \rangle - \langle \log(I_{\mathrm{G}}) \rangle$; where $\langle \log(I_{\mathrm{BPN}}) \rangle$ is the logarithmic mean transition ratio for bipolar nebulae. Sample numbers are typically $N = 500$ for the primary nebular sample, and $N = 40$ for the BPN (where we have used the listing of Phillips (1997) for BPN identification).

As a result, it is apparent that emission in BPN departs considerably from that of other planetary nebulae, with values I([OII]) exceeding those of the general population by a factor ~ 2.3. Such excesses are not however uniform,

and the enhancement in HeI ratios is considerably more modest (of order 7%).

The interpretation of such figures requires considerable caution since, as we have noted above, CNO processing of nebular material leads to anomalous abundances in type I/bipolar sources, whilst central star temperatures and shell masses are systematically higher than in the majority of PN. The procedure is also open to uncertainties regarding the mode of [OI] line formation, and possible variations in this mechanism between differing nebular sub-groups.

Where such excesses are interpreted primarily in terms of shocks, however, then it is possible to place relatively tight constraints upon shock parameters. In particular, a multi-dimensional least squares fit between the present results and the models of Hartigan et al. (1987) indicates that planar shocks with velocity $V_{\rm s} = 80 \Rightarrow 100$ km s^{-1} (models I80, I100 and B100) come closest to representing observed excesses. These trends, also illustrated in Fig. 6, follow observed variations reasonably closely; the most serious casualty ([NI]) reflecting probable enhanced N abundances in the BPN. Given that model grids are rather coarse, and that a small change in $V_{\rm s}$ by 20 km s^{-1} would cause order of magnitude variations in line ratios, it is unlikely that shock velocities will (in the mean) depart greatly from the values cited above.

How consistent is such a result with what is known of BPN shell kinematics? To assess this, we have illustrated a compilation of [OIII] and HI expansion velocities for the primary outflow shells (e.g. Kimeswenger 1997), together with maximum shell velocities from Corradi & Schwartz (1995) (Fig. 5); the latter corresponding to high velocity winds which may, in certain sources, be responsible for driving the lower velocity (higher mass) shells. It is clear, from this, that deduced shock velocities would be most consistent with higher shell outflow velocities $V_{\rm h}$ ($\langle V_{\rm h} \rangle =$ 161 km s^{-1}); primary shell velocities ($\cong$ 18 km s^{-1}) are too low. It is therefore conceivable that much of the excess emission arises through interaction between the differing kinematic outflow components.

4.2. Shocks associated with FLIERs

Recent investigations by Balick et al. (1993, 1994) have emphasised the unusual spectral characteristics of high velocity compact regions within the primary shells of planetary nebulae; features which these authors have dubbed FLIERs. Although it would be anticipated that the spectra of these components are dominated by shock excitation, Balick et al. have suggested that the observed ionisation structures are inconsistent with such a hypothesis, with [OI] peaking at larger radial distances than is the case for higher excitation lines. This conclusion would, in turn, be somewhat perplexing, given that there is so much other evidence to favour shock excitation; not least, in the clear similarity of the spectra to those of HH sources, and the difficulty in explaining these trends through any other mechanism. We shall here briefly attempt to resolve this paradox, before proceeding to investigate the spectral characteristics of nebulae in which FLIERs are found.

A linchpin in the analysis of Balick et al. (1994) is the assumption that the compact zones represent projections of post-shock cooling regimes in the plane of the sky - that is, that the observed ionisation stratification arises through post-shock cooling and recombination. This, in fact, is unlikely to be the case. On the basis of planar shock modelling, for instance, Hartigan et al. (1987) have noted that cooling zones would have typical widths

$$\Delta s = 5.8\ 10^{-5} \left[\frac{V_{\rm s}}{10^2\ {\rm km\ s^{-1}}}\right]^{4.67} \left[\frac{10^2\ {\rm cm^{-3}}}{n_{\rm p}}\right] {\rm pc}$$

for shock velocities $V_{\rm s} > 60$ km s^{-1}, where $n_{\rm p}$ is the pre-shock density of neutrals plus ions. Given $n_{\rm p} \sim 10^3$ cm^{-3} and $V_{\rm s} = 100$ km s^{-1} this would then imply $\Delta s \sim 5.8\ 10^{-6}$ pc, whilst bow shocks more consistent with typical FLIER velocities ~ 50 km s^{-1} would yield even lower values for Δs. It would appear, in brief, that the post-shock recombination zone is likely to be all but unresolvable, and that the physical dimensions of the FLIERs ($\sim$ .01 pc) correspond to the projected bow-shock structures themselves.

Viewed in this light, it can be seen that peak [OI] intensities would indeed be expected to occur where $V_{\rm s}$ is largest (e.g. Hartigan et al. 1987) - that is, at the location (the tip of the bow shock) where largest intensities appear actually to be observed.

A further query which concerns Balick et al. is the influence of ionisation by the central star radiation field; and it is certainly true that some post-shock ionisation of the cooling zone might be expected to lead to reduced low-excitation intensities. Here again, however, it is likely that the effect of this contribution can be greatly overstated. In particular, the flux of ionising photons at the location of most FLIERs is likely to be reduced through geometrical dilution, and the re-ionisation of neutral atomic species at lower radii. This, together with the appreciable post-shock densities expected for high M shocks, would presumably imply that radiative penetration of the post-shock cooling zone is likely to be very small indeed.

Taken as a whole, therefore, there seems little reason to doubt that the high velocity condensations of Balick et al. do indeed represent bow-shock features.

Given these circumstances, one may then reasonably ask whether such nebulae also possess excess lower excitation line strengths, as we have shown to be the case for BPN.

Such a trend, would, in fact be most unlikely, given that the shocked components appear to be highly compact, and contribute only a small proportion of the overall nebular spectrum; the primary nebular spectra are likely to be radiatively excited. Inspection of Figs. 1a largely confirms this expectation, revealing that most of the line

Table 3. Search for FLIERs in high-excitation nebulae

Source	Multiple Spectra?	Large Spec. Variation?	Image Resolved?	FLIERs?	Ref.
NGC 6537	N	-	Y	Y?	SCHW
IC 351	Y	N?	Y	Y?	IAC
HB 12	Y	N	N	-	IAC
NGC 2022	Y	N	Y	N	SCHW
M 2-23	N	-	N	-	P&K
Me 2-2	Y	N	N	-	IAC
NGC 6891	N	-	Y	N	IAC
NGC 6833	N	-	N	-	P&K
NGC 6790	N	-	N	-	SCHW
NGC 6879	N	-	Y	Y?	IAC
He 2-97	N	-	N	-	P&K
M 1-4	N	-	N	-	P&K
A 204A	N	-	-	-	-
A 204B	N	-	-	-	-
A 204C	N	-	-	-	-
J 320	Y	N	Y	Y	SCHW
NGC 6567	Y	N	Y	N	SCHW
NGC 5307	Y	N	Y	-	P&K
SN 1	N	-	Y	N	SCHW
M 1-1	N	-	N	-	IAC
M 2-30	N	-	N	-	P&K

intensities fall well outside of the shock regimes. Two further features are however well worth noting, and represent trends quite separate from the majority of sources.

It is apparent, in the first place, that relative line ratios are a highly variable function of position within the nebular shells - much more so than applies for most "normal" sources (viz. the connected line ratios for NGC 6543 and NGC 7009 in Figs. 1a). This, in turn, might be expected where observations are acquired at locations variously on and off the shock features.

A second characteristic of such sources is perhaps even more striking, and less open to anticipation.

Most of the line intensities for these sources, far from being located close to the shock regimes, appear to be in fact located at the opposite end of the excitation scale, and to contribute a very large fraction of the points at the lower limits of the [SII], [OI], [OII], [SIII] and [NI] line ratios (as well as clustering at the higher end of the HeII scale). Of the 25 nebulae having $\log([\mathrm{SII}]) \leq 0.4$ and $\log([\mathrm{OII}]) \leq 1.4$, for instance, fully 52% correspond to FLIER nebulae. The nebulae containing such high velocity features are clearly, in short, relatively high excitation sources, and it seems likely that the phenomenon of FLIERs must be in some way associated with this particular sub-category of nebula.

This, in turn, suggests that such spectral characteristics may represent a useful diagnostic tool in the search for further high velocity features.

The results of a provisional survey of this nature are summarised in Table 1, wherein we list all sources (excepting those of Balick et al. 1993, 1994) having $\log(10^2[\mathrm{OII}]/\mathrm{H}\beta) \leq 1.4$ and $\log(10^2[\mathrm{SII}]/\mathrm{H}\beta) \leq 0.4$. None of the nebulae possess widely disparate line ratios (as is the case with NGC 6543 and NGC 7009), although multiple spectra are available in only a few of the sources. Similarly, where nebular images are available in the catalogues of Schwartz et al. (1992; SCHW), Manchado et al. (1996; IAC), and Perek & Kohoutek (1967; P&K) only a minority are resolved.

Of the PN which have been adequately imaged, however, fully half show evidence for FLIER activity (J 320), shock structures (NGC 6537), or low excitation asymmetries and condensations which may be interpretable in terms of FLIERs (IC 351, NGC 6879). The other half possess broadly symmetric shells which may repay further investigation ; although it is apparent that all of these sources would benefit from a program of imaging at higher spatial resolutions, and in a broader range of transitions.

5. Conclusions

The structures of planetary nebulae are difficult to determine with any degree of reliability - and this, indeed, probably represents one of the primary obstacles to a full comprehension of their optical spectra. This apart, however, it is clear that spectra in most planetary nebulae can be simulated tolerably well through the application of comparatively simple models. Thus, in the present work, we have shown that [OII], HeI, and HeII intensities are all more or less consistent with what would be expected given radiative excitation, a spherical nebular structure, and a

broad range of central star temperatures, gas densities and (less critically) abundances.

Whilst higher excitation lines appear to possess relative strengths which are invariant with nebular radius, [OI], [SII], and [NI] are all shown to display evolutionary changes, together with an appreciable scatter which is likely to derive from variations in T_*, n_e, and the spectral sampling locations. The absence of comparable scatter in [OIII] and HeI (and the relative invariance of these line ratios) arises from a comparability of emission zones to that for HI, and relative insensitivity of emission coefficients to temperature and density.

In contrast to the other transitions, it appears that [OI] intensities exceed model predictions in the majority of nebulae. Such emission may arise through a variety of radiative processes associated (perhaps) with neutral shell components, including UV shadowing, charge-exchange reactions and so forth. In addition, we note that kinematic expansion velocities may be sufficient to trigger appreciable shock excitation of [OI]; a process which would explain the close correlation between [OI] and H_2 $S(1)$ line intensities.

Comparison between observed line ratios, and radiative and shock modelling trends also suggests that a suprisingly large proportion of [SII] λ6716/31 Å (approximately ~ 0.5 on average) may arise through shock excitation. This, of confirmed, would suggest that [SII] density estimates may be biassed towards the higher values characterising post-shock emission zones.

We have identified 14 nebulae in which shock emission may be appreciable, certain of which (CRL 618, M2-56) have previously been identified as shock sources on the basis of spectral diagnostics. A large proportion of these candidates appear also to be characterised by appreciable shocked H_2 $S(1)$ emission. It is suggested that differences in spectral line ratios between bipolar nebulae and the more general nebular sample may also derive from shocks; for which case, it is apparent that most BPN are likely to be shocked, and mean shock velocities would be of order $V_s = 80 \Rightarrow 100$ km s^{-1}. Such values appear consistent with observed BPN wind outflow velocities, implying that much of the observed excess may derive from interaction between high velocity winds and the very much slower primary shell outflows.

Sources containing FLIERs, on the other hand, appear to be located at the opposite end of the excitation scale, and are confined to extremely tightly defined spectral regimes; of the spectral measurements having $\log(10^2[\mathrm{OII}]/\mathrm{H}\beta) \leq 1.4$ and $\log(10^2[\mathrm{SII}]/\mathrm{H}\beta) \leq 0.4$, approximately 52% correspond to sources associated with FLIERs. This characteristic suggests a new diagnostic for the identification of further such outflows; a methodology which has been applied to suggest possible FLIER activity in NGC 6537, NGC 6879, IC 351 and (in particular) J320, where various symmetrically disposed pairs of condensations straddle the nucleus and dominate the low excitation structure.

References

Aller L.H., 1982, ASS 83, 225
Balick B., Preston H.L., Icke V., 1987, AJ 94, 1641
Balick B., Perinotto M., Maccioni A., Terzian Y., Hajian A., 1994, ApJ 424, 800
Balick B., Rugers M., Terzian Y., Chengalur J.N., 1993, ApJ 411, 778
Boeshaar G.O., 1974, ApJ 187, 283
Boffi F.R., Stanghellini L., 1994, A&A 284, 248
Bohigas J., 1994, A&A 288, 617
Cahn J.H., Kaler J.B., Stanghellini L., 1992, A&AS 94, 399
Capriotti E.R., 1973, ApJ 179, 495
Corradi R.L.M., Schwartz H.E., 1995, A&A 293, 871
Cuesta L., Phillips J.P., Mampaso A., 1993, A&A 267, 199
Cuesta L., Phillips J.P., Mampaso A., 1995, A&A 304, 475
Goodrich R.W., 1991, ApJ 376, 654
Gruenwald R.B., Viegas S.M., 1992, ApJS 78, 153
Harrington P., 1995, STScI Press Release STScI-PRC95-01
Hartigan P., Raymond J., Hartmann L., 1987, ApJ 316, 323
Hyung S., Aller L.H., 1996, MNRAS 278, 551
Hyung S., Aller L.H., 1995, MNRAS 273, 973
Hyung S., Aller L.H., Feibelman W.A., 1994, MNRAS 269, 975
Hyung S., Keyes C.D., Aller L.H., 1995, MNRAS 272, 49
Icke V., Balick B., Frank A., 1992, A&A 253, 224
Icke V., Preston H.L., 1989, A&A 211, 409
Kaler J.B., Browning L.B., Shaw R.S., 1996, A Catalog of Relative Emission Line Intensities in Planetary Nebulae
Kastner J.H., Gatley Y., Merrill K.M., Probst R., Weintraub D.A., 1994, ApJ 421, 600
Kastner J.H., Weintraub D.A., Gatley Y., Merrill K.M., Probst R., 1996, ApJ 462, 777
Kimeswenger S., 1997, The Data Base of Galactic PNe in Innsbruck, Institute of Astronomy, Innsbruck
Kingsburgh R.L., Barlow M.J., 1992, MNRAS 257, 317
Kingsburgh R.L., English J., 1992, MNRAS 259, 635
Köppen J., 1979, A&A 80, 42
Köppen J., 1983, A&A 122, 95
Lopez J.A., Vazquez R., Rodriguez L.F., 1995, ApJ 455, L63
Mallik D.C.V., Peimbert M., 1988, Rev. Mex. A&A 16, 111
Manchado A., Guerrero M.A., Stanghellini L., Serra-Ricart M., 1996, IAC Morphological Catalog of Northern Galactic Planetary Nebulae, IAC
Meaburn J., Walsh J.R., 1980a, MNRAS 257, 628
Meaburn J., Walsh, J.R., 1980b, MNRAS 193, 631
Middlemass D., 1990, MNRAS 244, 294
O'Dell C.R., Handron K.P., 1996, STScI Press Release STScI-PR96-13
Peimbert M., Torres-Peimbert S., 1983, in Planetary Nebulae, IAU Symp. 103, Flower (ed.), p. 233
Perek L., Kohoutek L., 1967, Catalogue of Galactic Planetary Nebulae, Academa Publ. House, Czechoslovak Academy of Sciences
Phillips J.P., 1989, in: Planetary Nebulae, IAU Symp. 131, Torres-Peimbert S. (ed.), p. 425
Phillips J.P., 1997, A&A (in press)
Phillips J.P., Reay N.K., 1980, Astrophys. Lett. 21, 47

Phillips J.P., Williams P.G., Mampaso A., Ukita N., 1992, ASS 188, 171
Pottasch S.R., 1984, Planetary Nebulae. D. Reidel Publishing Co., Dordrecht, Holland
Raymond J.C., Hartigan P., Hartmann L., 1988, ApJ 326, 323
Reay N.K., Walton N.A., Atherton P.D., 1988, MNRAS 232, 615
Rowlands N., Houck J.P., Hertier T., 1994, ApJ 427, 867
Savage B.D., Mathis J.S., 1979, ARA&A 17, 73
Schwartz H.E., Corradi R.L.M., Melnick J., 1992, A&AS 96, 23
Schonberner D., 1979, A&A 79, 108
Schonberner D., 1981, A&A 103, 119
Schonberner D., 1983, A&A 272, 708
Shull M.J., McKee C.F., 1979, ApJ 227, 131
Trammell S.R., Goodrich R.W., 1996, ApJ 468, L107
Tylenda R., Acker A., Stenholm B., Köppen J., 1992, A&AS 95, 337
Webster B.L., Payne P.W., Storey J.W.V., Dopita M.A., 1988, MNRAS 235, 533
Zuckerman B., Gatley Y., 1988, ApJ 324, 501